Synthesis of Polymer-Coated Magnetic Nanoparticles to the Surface of Activated Carbon and Kinetic Studies

Huseyn OSMAN [1] iD, Mehmet UGURLU [1*] iD, Ali Imran VAIZOGULLAR [2] iD, Selman Ilteris YILMAZ [3] iD, Abdul Jabbar CHAUDHARYD [4] iD

[1] Department of Chemistry, Faculty of Science, Mugla Sitli Kocman University, 48000, Mugla, Turkey

[2] Vocational School Healthcare Med Lab Program, Mugla Sitli Kocman University, 48000, Mugla, Turkey

[3] Vocational School of Technical Sciences, Biomedical Technology Program, Istanbul University-Cerrahpasa, 34500, Istanbul, Turkey

[4] Department of Life Sciences, Division of Environmental Sciences, Brunel University London, UB8, 3PH, UK

Corresponding author E-mail: mehmetu@mu.edu.tr

H I G H L I G H T S

> The effect of polymer-coated magnetic nanomaterials.
> Recycling of adsorbents after use and their usability in wastewater treatment.
> Gaining magnetic properties of FeO, Fe_2O_3 or Fe_3O_4 and metal oxides to the activated carbon surface with polymeric materials.

A B S T R A C T

In the presented study, it was investigated the synthesis of activated carbon (AC), magnetic activated carbon (MagAC), styrene-butadiene styrene magnetic activated carbon (SBS/MagAC) and poly charbonat magnetic activated carbon (PC/MagAC) samples. Thermogravimetric Analyzer (TGA), Differential Scanning Calorimeter (DSC), Scanning Electron Microscope (SEM), X-Ray Diffractometer (XRD), Fourier Transform Infrared Spectrophotometer (FTIR analysis), Brunauer-Emmett-Teller (BET) analysis were used for characterization studies. Adsorbent type, temperature, solid-liquid ratio, initial concentrations and solution pH were selected as parameters in experiments. The experimental study was carried out at low pH yields were higher and performance was 98-99% in AC and Mag/AC samples. It was found that the polymer coated magnetic materials did not perform very well at high pH. It was also seen that MagAC and SBS/MagAC are more effective than AC and PC/MagAC to remove phenol.

1. Introduction

Phenol (C_6H_5OH), an aromatic compound, is one of the 126 most toxic chemicals and is very dangerous, harmful, and causes excretion of dark urine, impaired vision, diarrhea and sour mouth. Marine life additionally tends to be disturbed by the chemical phenol due to its toxic nature.

The effective removal of these pollutants from wastewater is a problem of great importance and interest. Great research efforts on adsorption processes and adsorbent materials for separating organic pollutants from waste streams have been developed. Phenol is obtained from coal tar or benzene. It is a common pollutant in wastewater as a result of its widespread use in different industrial fields (pharmaceutical, steel, textile industry, plastics, dyestuff, paper, epoxy, phenolic resin, pesticide, insecticide, petroleum refinery, coal gasification, olive water, etc.) [1,2].

The simple and effective way can be used to remove organic pollutant and also recycling, recover and reuse adsorbent materials. When the literature studies are

examined, it is seen that the adsorption method is mostly preferred and used for phenol removal. However, it is stated that new methods, especially by using activated carbon-based materials, can provide different results and selectivity for phenol with nano-based materials. The application of magnetic particle technology to solve environmental problems has received considerable attention. Magnetic particles can be used to adsorb contaminants from aqueous or gaseous effluents and after adsorption, can be separated from the medium by a simple magnetic process. Examples of this technology are the use of magnetite particles to accelerate the coagula of sewage [3,4]. The samples of activated carbon (AC) coated with magnetically iron-containing iron components (FeO. γ-Fe_2O_3 or Fe_3O_4) have recently been used to remove toxic organic [5,6]. Cr(VI) [7], different heavy metals [8], antibiotics [9] and As (V) [10] to purify effluent streams using adsorption method. These new adsorbent materials can be used for different purposes after being coated with certain polymeric materials. In the literature, it has been stated that the chemical bond with mercury on the activated carbon surface may be the result of Hg-Cl and Hg-S interactions [11]. In the presented study, especially the phenol with toxic pollution was tried to be removed, taking into account that magnetic nanomaterials can be easily removed from the aqueous environment. The reason for using activated carbon material is better loading of the magnetic material, the height of the surface area and then the easy feasibility of recovering the adsorbent in the magnetic field. In addition, their characterization and other structural properties were investigated.

2. Materials and method

Commercially available Activated carbon samples were used in all experimental studies. These examples were provided as "Sigma-Aldrich 242276". The Iron salts were commercially available (ZAG, ZK.100380.1000) and were prepared according to literature studies [12]. In the presented experimental study, three different adsorbents were prepared and used. $FeCl_3$ (1.08 g) and $FeCl_2$ (2.40 g) and 150 ml distilled water were added as the first adsorbent. For the second sample, SBS (1 g) + THF/DMF 50ml (30:20) samples were prepared. The third sample was PC (1 g) and THF/DMF 50ml (30:20) samples. Then, after these samples were stirred at 60-65°C for 2 hours, $FeCl_3$ (1.08 g) and $FeCl_2$ (2.40 g) were added to them. Then, 5 g of NaOH was added and mixed for 1 hour and left overnight. It was washed several times with distilled water and then filtered and dried in an oven to constant weight. These examples are called Mag/AC, SBS/MagAC, and PC/MagC.

2.1. Characterization of nanoparticle material

Perkin-Elmer Lambda 35 UV-Vis Spectrophotometer for UV-Vis absorbance, Perkin-Elmer Pyris 1 Thermogravimetric Analyzer for TGA analysis, Perkin-Elmer Diamond Differential Scanning Calorimeter for DSC analysis, Scanning Electron Microscope for SEM images (JSM 7600). Rigaku-Smart-Lab-X-Ray Diffractometer for XRD analysis, Thermo Scientific. Nicolet Is10. Fourier Transform Infrared Spectrophotometer for FTIR analysis and Micromeritics TriStar II PLUS for Brunauer-Emmett-Teller (BET) analysis were used for characterization studies.

3. Results and Discussion

Characterization of materials synthesized by using different polymer materials constitutes an important part of the study. Considering this situation, the samples of all three nanomaterials (AC, MagAC, SBS/MagAC and PC/MagAC) Structural and characterization were investigated by various analytical techniques such as FTIR, SEM, EDS, XRD, TGA, DSC and BET. The obtained data were tried to be evaluated by considering similar studies. the results are given below in order.

3.1. SEM/EDS images and BET Analysis

SEM and EDS results have an important place in order to see closely the surface topography, morphological structures of the prepared materials and the general states of the atoms or molecules in the structure formed when coated with polymeric material. These data are given in Figure 1 below.

SEM images of activated carbon samples show a porous structure with a clear porosity. The porous structure here is evident with many cavities, recessed and protruding forms on the outer surface. On the other hand, in MagAC and PC/MagAC, it is observed that there may be more dull and clear aggregation. This suggests that the magnetic material adheres to the porous surfaces and the pores of the adsorbent. SEM images of the SBS/MagAC material are shown in figure 1c. Here, it is seen that the polymeric material leads to more aggregation. More agglomeration, especially in the surface topography, can be associated with significant diffusion of polymers into the pores of the activated carbon. When the EDS analyzes of the adsorbent materials are examined, too much Ca, Fe, C and O elements are observed here, not only on the AC surface. A very limited situation is seen on the AC surface. it is seen that it contains small amounts of Na and Mg elements. In addition, trace amounts of Cu and Si elements are observed in SBS/MagAC material. In the BET surface area measurement, the surface areas of AC and synthesized materials are generally as AC (687.751 m^2g^{-1}) > MagAC (636.86 m^2g^{-1}) > PC/MagAC (304.56 m^2g^{-1}) > SBS/MagAC (251.31m^2g^{-1}) distribution.

3.2. XRD Images

Figure 2 shows the XRD pattern of the polymeric materials with activated carbon support.

As seen from the Figure 2, the 2-theta degree of no treated activated carbon with sharply 20.82°, 26.42°, 29.37°, 42.82° and 62.26° peaks are seen in the sample confirming the homogeneous and regular crystal structure. The peaks at 26.42° and 42.82° presented the (002) and (100) planes respectively. Also, the 26.42° diffraction peak displays the growing of AC on the direction of the (002) surface [13]. In addition, the XRD pattern of other samples were examined, the peak intensity and some crystallite changings were observed suggesting the transforming of crystal structure to amorphous timely. In a word, the FWHM values were wider than that of other AC support samples. It can be concluded that particle size and amorphous phenomenon decrease [14].
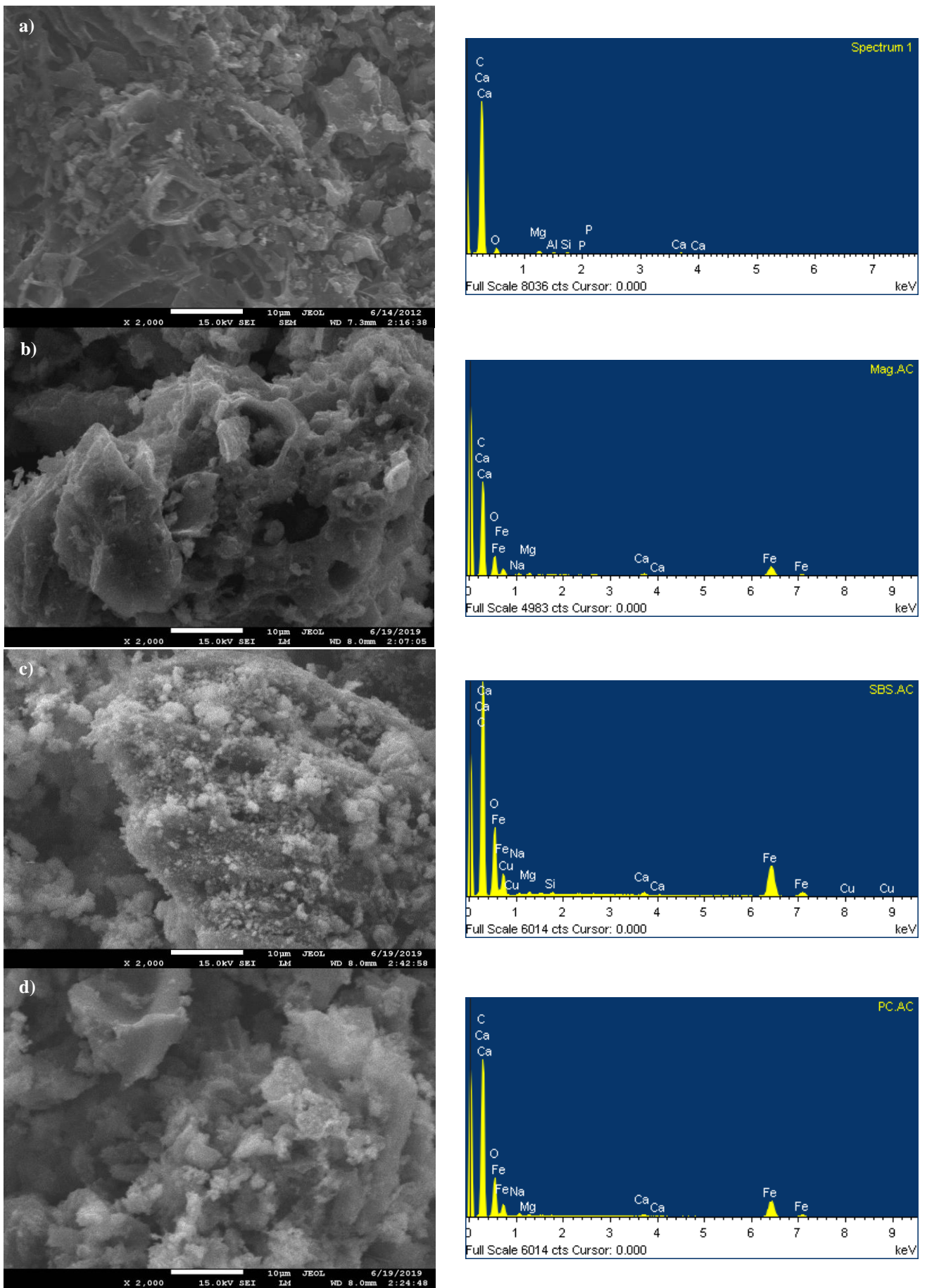
Fig. 1. SEM and EDS images of adsorbent materials a) AC, b) MagAC, c) SBS/MagAC, d) PC/MagAC
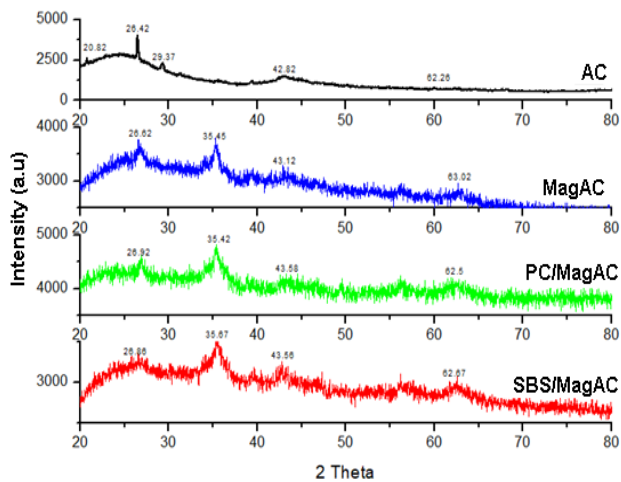
Fig. 2. XRD images of different adsorbent materials

In MagAC, the diffraction peak at 35.45° with iron components was observed with together AC diffraction peaks. These results strongly show that iron components during the synthase with treatment of strong base participated of all iron ions. The crystallite structure of PC and SBS was not changing on iron based components. As seen in SBS/MagAC diffraction peaks, FWHM values increased with decreasing of peak intensity indicating an effective size distribution of SBS on AC support. All XRD pattern presented that AC support polymeric materials were synthesized efficiently and effective dispersion of magnetic/polymeric components on AC support.

3.3. TGA analysis

TGA analysis of the samples prepared using activated carbon-based and different polymeric materials and the relationship between temperature and mass loss was investigated. Obtained results are given in Figure 3.
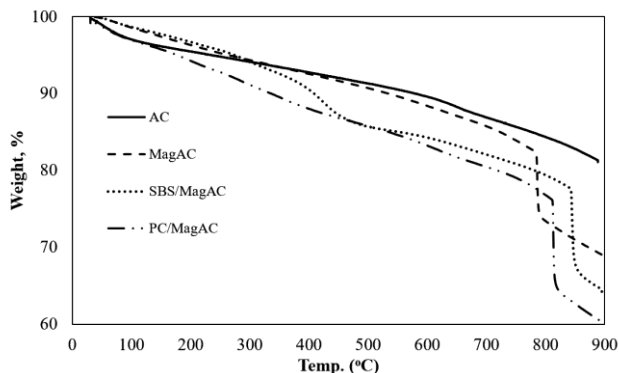

Fig 3. TGA results of AC, MagAC, BS/MagAC, and PC/MagAC adsorbents

In short, TGA is a method studied to examine the ability of a substance to maintain its mass (thermal stability) under different conditions. In an other saying, it is the continuous monitoring of the changes in the mass of the substance depending on as function of the temperature. As seen from Fig 3, it is seen that the TGA values of AC generally lose mass with increasing temperature and a significant peak change occurs. Here, a significant peak change was appeared at MagAC and PC/MagAC samples at approximately 800°C and at the other SBS/MagAC samples

at 850°C. This can be explained that the thermogravimetric method is dynamic that the system will never reach equilibrium and that changes in the amorphous and crystalline structure can occur with increasing temperature [15]. It can be said in general from all the data that mass loss was evident and sharp in all adsorbents starting from 800 °C. This is particularly explained to the decomposition and change of the carbon skeleton found in polymer-coated materials [16].

3.4. DSC analysis

DSC analysis of the samples prepared using activated carbon-based and different polymeric materials, the relationship between temperature and mass loss was investigated. Obtained results are given in Figure 4.
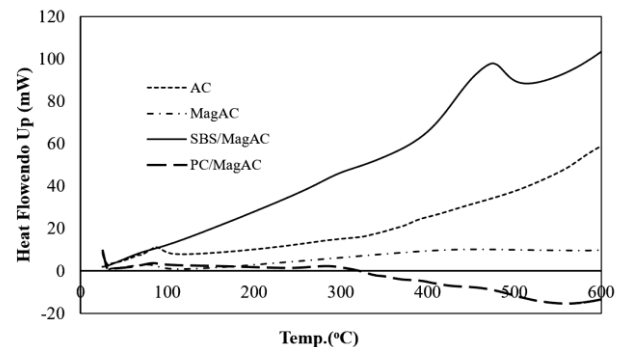

Fig. 4. DSC results of AC, MagAC, SBS/MagAC and PC/MagAC adsorbents

The DSC method is widely used in the research and development, process optimization and quality monitoring of plastics, rubber, coatings, pharmaceuticals, catalysts, inorganic materials, metal materials and composite materials. DSC analyses are preferred for thermal stability and oxidative stability of the material in different atmospheres, physical and chemical processes such as decomposition, adsorption, desorption, oxidation and reduction, and further reaction kinetics. Here are the experimental factors that affect the analysis and measurement. Factors such as temperature increase, sample dosage, particle size, convection, turbulence and sample tightness have significant effects. In the DSC process, the temperature of all sample and reference is increased at a regular rate by measuring the amount of energy absorbed or released while the sample is heated and cooled or kept at a constant temperature. When endothermic heat is applied to the sample simultaneously, on the other hand, there is heat transfer to the outside at the same time, where an esothermic drum is observed. In this process, the losses and gains in the sample are realized. Here, the heating of the sample appears as a function of temperature. When examined in Figure 4, it is observed that endothermic peaks occur around 100°C in AC samples. An exothermic peak of the MagAC sample was formed and increased by being affected by the temperature. Exothermic peaks are observed at 500°C in SBS/MagAC samples, and endothermic peaks are observed in PC/MagAC samples at 100°C and 300°C. Significant changes were observed specially in SBS/MagAC samples. in others, very significant changes were observed to be limited.
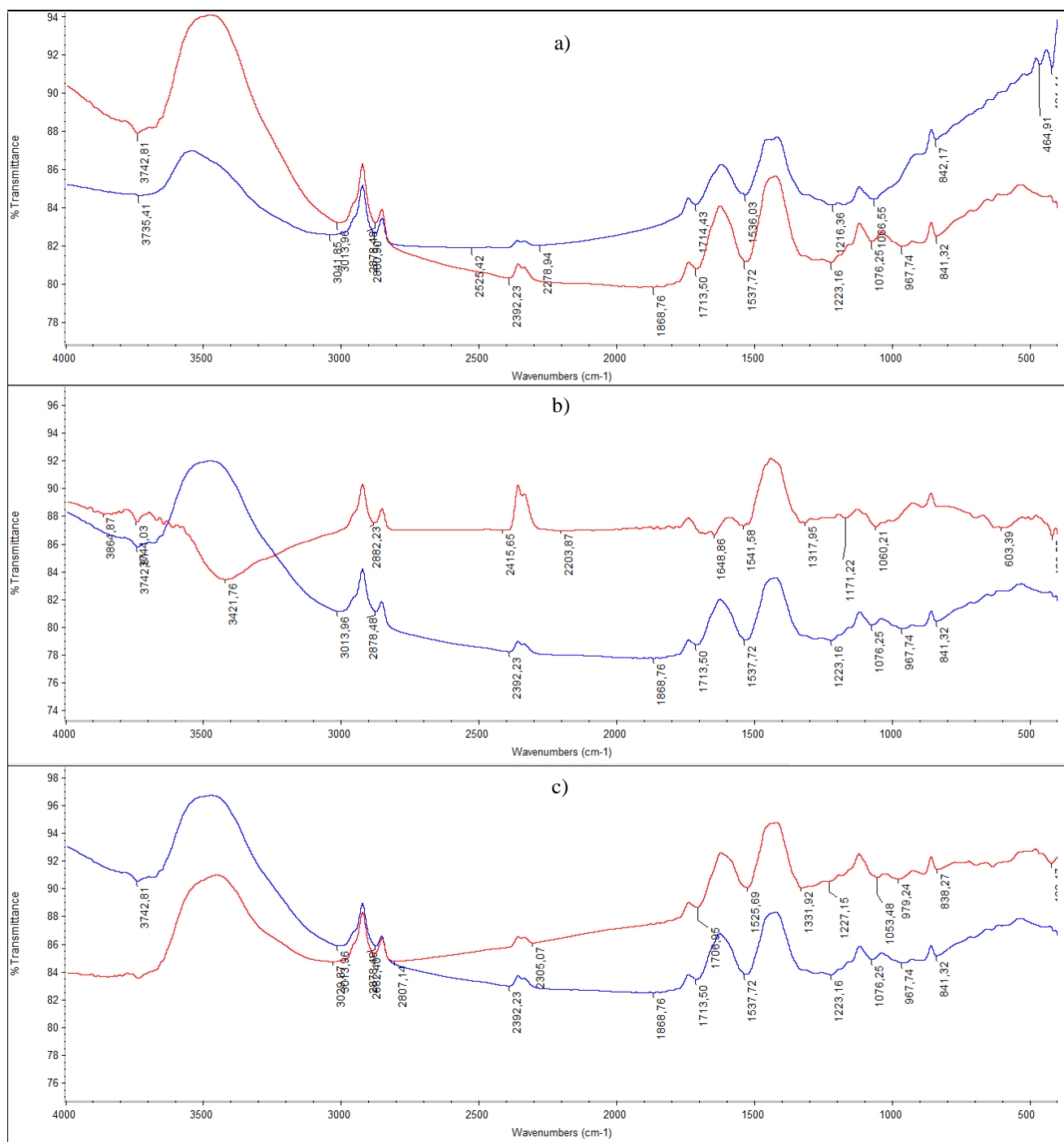
Fig. 5. FT-IR results a) AC vs MagAC, b) AC vs PC/MagAC, c) AC vs SBS/MagAC adsorbents

3.5. FT-IR Images

FT-IR spectra of polymeric coated magnetic materials using activated carbon samples are given in Fig.5.

Figure 5, shows the FTIR spectra of the adsorbent samples. As seen from the Figure 5, the –OH peak at 3041.85 cm^{-1} of AC presented the interactions of Fe$_3$O$_4$ confirming a shifting to 3013.96 cm^{-1}. This is indicating an effective physical interaction on the OH groups. The shifting of 1216.36 cm^{-1} peak to 1223.16 cm^{-1}, displays the C-O bond attached with –OH group. The C-H, C=O and C = C peaks was seen at 2880.90 cm^{-1}, 1714.43 cm^{-1} and shrinkage 1536.03 cm^{-1} peaks respectively. This is explained that no interactions were observed with these peaks. The PC based AC with interaction of Fe$_2$Fe$_3$O$_4$ exhibited the shifting of OH peak from 3019.96 cm^{-1} to 3421.76 cm^{-1}. This is suggested that the hydrogen bonds between -COO group and –OH molecules caused during the synthesized of PBS/MagAC. Also, the C=O bond seen at 1648.86 cm^{-1} confirmed this reality. With the connecting of hydrogen bond decreased the peak intensity at 1648.86 cm^{-1}. The 603.39 cm^{-1} peak in polycarbonate-bonded MagAC composite material was not showed the Fe-C bond in MagAC sample. In addition, the peak of C-O bond at 1223.16 cm^{-1} in Mag/AC sample showed the less interactions between polycarbonate and MagAC with confirming the 1171.22 cm^{-1} peak. Also, the IR spectra of the polymeric samples obtained with Fe$_2$Fe$_3$O$_4$ coated activated carbon was seen [17,18].

Table 1a. In phenol adsorption of AC and Mag AC and I. II. degree kinetic model and particle diffusion data

Parameters	AC									MagAC								
	First-order	Pseudo-second-order				Intra-particle diffusion				First-order	Pseudo-second-order				Intra-particle diffusion			
	R^2	$q_{e(calcul)}$ (mgg⁻¹)	$q_{e(exp)}$ (mgg⁻¹)	$k_2 \times 10^{-3}$ (g/mgmin)	R^2	k_1 (g/mgmin)	C	R^2	$t_{1/2}$ (min)	R^2	$q_{e(calcul)}$ (mgg⁻¹)	$q_{e(exp)}$ (mgg⁻¹)	$k_2 \times 10^{-3}$ (g/mgmin)	R^2	k_1 (g/mgmin)	C	R^2	$t_{1/2}$ (min)
Ads. dos. (gL⁻¹)																		
0.5	0.90	196.07	186.98	0.5	0.99	8.58	86.15	0.89	10.70	0.88	169.49	163.35	1.00	0.99	6.74	89.74	0.77	6.12
1.0	0.84	153.84	147.21	0.8	0.99	7.09	68.36	0.72	8.49	0.84	185.18	162.33	0.20	0.99	12.26	12.12	0.93	30.80
2.0	0.85	78.74	72.91	0.8	0.99	4.40	20.79	0.93	17.14	0.86	101.01	87.21	0.05	0.99	6.53	13.97	0.89	22.93
Temp. (K)																		
291	0.79	51.28	44.50	0.9	0.98	2.88	4.37	0.94	24.97	0.88	76.33	38.50	0.3	0.87	3.82	6.46	0.93	6.58
298	0.88	36.10	36.45	0.8	0.99	0.43	29.01	0.91	34.29	0.74	34.36	34.07	11.1	0.99	0.44	28.54	0.85	2.67
308	0.82	34.36	34.41	11	0.99	3.21	6.16	0.96	2.64	0.81	33.33	34.01	6.01	0.99	0.39	27.09	0.72	4.90
Initial Con.(mgL⁻¹)																		
125	0.85	46.94	46.16	3.0	0.99	3.21	6.16	0.96	7.22	0.84	40.81	40.70	0.41	0.99	1.01	27.18	0.95	61.43
250	0.70	70.42	70.91	5.1	0.99	0.66	27.71	0.75	2.82	0.85	68.49	68.14	7.01	0.99	0.90	57.61	0.85	2.10
500	0.77	135.13	134.01	3.1	0.99	0.40	29.12	0.91	2.49	0.85	129.87	128.20	3.03	0.99	1.31	111.48	0.88	2.60
Initial pH																		
3.0	0.86	38.46	35.66	1.35	0.98	1.94	11.09	0.97	28.04	0.87	24.75	24.48	4.04	0.99	0.89	13.20	0.96	10.21
5.0	0.77	39.21	36.99	1.10	0.98	1.91	13.17	0.98	27.03	0.87	27.70	25.06	2.02	0.98	1.57	6.23	0.95	19.95
7.0	0.86	40.16	36.41	1.21	0.98	2.25	8.76	0.97	27.46	0.86	19.76	18.90	4.01	0.99	0.99	7.17	0.89	13.23
9.0	0.58	38.16	34.94	1.12	0.98	2.03	10.69	0.94	28.62	0.86	11.45	10.29	5.02	0.99	0.83	0.77	0.83	19.44

Table 1b. Phenol adsorption. SBS / MagAC and PC / MagAC I.II.degree kinetic model and particle diffusion data

| Parameters | SBS/MagAC | | | | | | | | | PC/MagAC | | | | | | | | |
| | First-order | Pseudo-second-order | | | | Intra-particle diffusion | | | | First-order | Pseudo-second-order | | | | Intra-particle diffusion | | | |
	R^2	$q_{e(calcul)}$ (mgg^{-1})	$q_{e(exp)}$ (mgg^{-1})	$k_2 \times 10^{-3}$ (g/mgmin)	R^2	k_I (g/mgmin)	C	R^2	$t_{1/2}$ (min)	R^2	$q_{e(calcul)}$ (mgg^{-1})	$q_{e(exp)}$ (mgg^{-1})	$k_2 \times 10^{-3}$ (g/mgmin)	R^2	k_I (g/mgmin)	C	R^2	$t_{1/2}$ (min)
Ads. dos. (gL^{-1})																		
0.5	0.85	200.00	183.77	0.03	099	11.78	44.58	0.92	181.39	0.85	188.67	168.37	0.2	0.97	10.81	35.78	0.96	27.21
1.0	0.85	185.18	156.28	0.01	0.96	12.74	2.79	0.93	639.88	0.88	144.92	122.14	0.2	0.99	9.37	9.36	0.94	31.99
2.0	0.82	84.74	63.93	0.03	0.98	5.61	4.39	0.95	521.40	0.85	120.48	50.58	0.2	0.97	4.86	11.84	0.94	78.21
Temp. (K)																		
291	0.77	31.05	24.08	10.1	0.98	2.15	1.68	0.94	4.11	0.86	45.45	30.52	0.06	0.97	2.88	4.37	0.94	6.14
298	0.75	27.39	27.03	11.0	0.99	0.44	21.59	0.87	3.36	0.86	29.15	28.66	13	0.99	0.45	23.59	0.86	2.85
308	0.56	24.57	24.92	100	0.99	0.03	24.76	0.87	0.40	0.82	26.88	27.55	17	0.99	0.57	25.44	0.89	2.36
Initial Conc.(mgL^{-1})																		
125	0.82	29.23	29.19	16	0.99	0.52	23.19	0.66	2.14	0.86	34.12	33.90	0.8	0.99	0.69	25.40	0.92	42.82
250	0.86	56.49	55.94	4.2	0.99	1.07	42.40	0.95	4.26	0.82	58.13	57.33	7.0	0.99	0.76	48.58	0.72	2.55
500	0.81	140.84	139.94	3.1	0.99	1.54	121.37	0.94	2.31	0.86	126.58	126.22	2.0	0.99	2.19	97.61	0.95	3.57
Initial pH																		
3.0	0.75	24.27	14.50	1.0	0.86	1.46	3.14	0.94	68.97	0.82	28.01	27.57	6.0	0.99	0.76	18.23	0.94	11.49
5.0	0.86	36.49	18.73	0.6	0.95	1.85	3.70	0.95	88.98	0.80	31.25	30.64	4.0	0.99	1.02	18.04	0.96	13.35
7.0	0.85	20.53	14.83	1.6	0.94	1.50	2.39	0.91	42.14	0.85	27.54	26.57	4.0	0.99	0.98	14.49	0.94	16.86
9.0	0.86	4.79	3.65	6.1	0.98	0.29	0.23	0.97	44.91	0.80	19.96	18.78	5.0	0.99	1.03	7.26	0.84	54.79

3.6. Adsorption Kinetics

The modified adsorbents are potential adsorbents due to their non-toxicity and efficiency. They contain chemically active functional groups that serve as efficient sites to bind adsorbents. The functional groups present in modified AC have affinity for removal phenol such as chemisorption, complexation, adsorption on surface. To obtain the kinetics of the phenol adsorption process on all adsorbents. Three kinetic models were studied (i.e. pseudo-first-order. pseudo-second-order and intra-particle diffusion kinetic models). The obtained results are shown in Table 1a and Table 1b.

When the data obtained from this study were evaluated, it was seen that the pseudo-first order model for all adsorbents was not suitable for seeing the interaction between phenol and all adsorbents due to lower R^2 values (0.56-0.90) and smaller theoretical q_e values. When the R^2 value obtained from the intraparticle diffusion model is examined, it is in the range of 0.72-0.96 and is false-second (0.99). The R^2 value obtained from the intraparticle diffusion model is in the range of 0.72-0.96 and is pseudo-second order (0.99). These results showed that adsorption of phenol on AC and magnetic materials followed pseudo second order in all parameters examined. The higher R^2 value of the intraparticle diffusion kinetics indicates that the ongoing adsorption process can also conform to the intraparticle diffusion kinetics. The theoretical q_e values (from the so-called second order model) are close to the values obtained from the experimental results which further confirms their suitability. In this case the adsorption process of phenol can be described as chemisorption and the rate determination step is suggested to be surface adsorption. Given the intraparticle diffusion model it can be said that there is a close agreement between the experimental and theoretical q_e value confirming the applicability of this model to explain phenol adsorption by all adsorbents. This shown that surface adsorption and intraparticle diffusion occur simultaneously. This can be mainly attributed in two stages firstly the outer surface of the adsorbents and later one the diffusion into the pores [19].

4. CONCLUSION

From The presented study, it was seen that AC, MagAC, SBS / MagAC and PC / MagAC can be used as good adsorbents to remove high phenol matter from wastewater. Different characterization study was investigated for the structural characterization of adsorbents such as; Scanning electron microscopy (SEM), X-ray diffraction (XRD) analysis and Brunauer Emmett Teller (BET) measurements. Adsorption kinetics were conducted to investigate the adsorption potential of all adsorbents for phenol removal. The kinetic models appeared that the adsorption process onto adsorbents at all temperatures obeyed pseudo-second-order and intra-particle diffusion models rather than the pseudo-first-order kinetic model (R^2: 0.98-1.00). It has been seen that the efficiency realized in the whole adsorption can be realized as AC ≥ MgAC ≥ PC/MagAC ≥ SBS/MagAC samples, respectively. As a result, although higher efficiency is obtained with AC, it is observed that phenol can be removed from the aqueous environment more easily, especially when magnetic and polymeric materials are studied.

Acknowledgements

Compliance with Ethical Standards

There is no conflict of interest to disclose.

Conflict of Interest

The author(s) declares no known competing financial interests or personal relationships that could have appeared to influence the work reported in this paper.

References

1. Adar, E.; Atay, İ.N.; Büncü, K.; Bilgili, M.S. Phenol removal from synthetic wastewater with powdered activated carbon: Isotherms, kinetics and thermodynamics. *Environmental Research and Technology* **2020**, *3*, doi:10.35208/ert.692302.

2. Khalid, M.; Joly, G.; Renaud, A.; Magnoux, P. Removal of Phenol from Water by Adsorption Using Zeolites. *Industrial & Engineering Chemistry Research* **2004**, *43*, 5275–5280, doi:10.1021/ie0400447.

3. Hamad, H.T. Removal of phenol and inorganic metals from wastewater using activated ceramic. *Journal of King Saud University - Engineering Sciences* **2021**, *33*, 221–226, doi:10.1016/j.jksues.2020.04.006.

4. Akın, D.; Yakar, A.; Gündüz, U. Synthesis of Magnetic Fe3O4-Chitosan Nanoparticles by Ionic Gelation and Their Dye Removal Ability. *Water Environment Research* **2014**, *87*, 425–436, doi:10.2175/106143014x14062131178673.

5. Bagheri, A.R.; Ghaedi, M.; Asfaram, A.; Bazrafshan, A.A.; Jannesar, R. Comparative study on ultrasonic assisted adsorption of dyes from single system onto Fe3O4 magnetite nanoparticles loaded on activated carbon: Experimental design methodology. *Ultrasonics Sonochemistry* **2017**, *34*, 294–304, doi:10.1016/j.ultsonch.2016.05.047.

6. Bhatia, D.; Datta, D.; Joshi, A.; Gupta, S.; Gote, Y. Adsorption Study for the Separation of Isonicotinic Acid from Aqueous Solution Using Activated Carbon/Fe3O4 Composites. *Journal of Chemical & Engineering Data* **2018**, *63*, 436–445, doi:10.1021/acs.jced.7b00881.

7. Gong, K.; Hu, Q.; Yao, L.; Li, M.; Sun, D.; Shao, Q.; Qiu, B.; Guo, Z. Ultrasonic Pretreated Sludge Derived Stable Magnetic Active Carbon for Cr(VI) Removal from Wastewater. *ACS Sustainable Chemistry & Engineering* **2018**, *6*, 7283–7291, doi:10.1021/acssuschemeng.7b04421.

8. Zhang, S.; Wang, Z.; Chen, H.; Kai, C.; Jiang, M.; Wang, Q.; Zhou, Z. Polyethylenimine functionalized Fe3O4/steam-exploded rice straw composite as an efficient adsorbent for Cr(VI) removal. *Applied Surface Science* **2018**, *440*, 1277–1285, doi:10.1016/j.apsusc.2018.01.191.

9. Badi, M.Y.; Azari, A.; Pasalari, H.; Esrafili, A.; Farzadkia, M. Modification of activated carbon with magnetic Fe3O4 nanoparticle composite for removal of ceftriaxone from aquatic solutions. *Journal of Molecular Liquids* **2018**, *261*, 146–154, doi:10.1016/j.molliq.2018.04.019.

10. Wen, T.; Wang, J.; Yu, S.; Chen, Z.; Hayat, T.; Wang, X. Magnetic Porous Carbonaceous Material Produced from Tea Waste for Efficient Removal of As(V), Cr(VI), Humic Acid, and Dyes. *ACS Sustainable Chemistry & Engineering* **2017**, *5*, 4371–4380, doi:10.1021/acssuschemeng.7b00418.

11. Kim, E.-A.; Seyfferth, A.L.; Fendorf, S.; Luthy, R.G. Immobilization of Hg(II) in water with polysulfide-rubber (PSR) polymer-coated

activated carbon. *Water Research* **2011**, *45*, 453–460, doi:10.1016/j.watres.2010.08.045.

12. Fard, M.A.; Vosoogh, A.; Barkdoll, B.; Aminzadeh, B. Using polymer coated nanoparticles for adsorption of micropollutants from water. *Colloids and Surfaces A: Physicochemical and Engineering Aspects* **2017**, *531*, 189–197, doi:10.1016/j.colsurfa.2017.08.008.

13. Girgis, B.S.; Temerk, Y.M.; Gadelrab, M.M.; Abdullah, I.D. X-ray Diffraction Patterns of Activated Carbons Prepared under Various Conditions. *Carbon letters* **2007**, *8*, 95–100, doi:10.5714/CL.2007.8.2.095.

14. Vaizoğullar, A.İ. TiO2/ZnO Supported on Sepiolite: Preparation, Structural Characterization, and Photocatalytic Degradation of Flumequine Antibiotic in Aqueous Solution. *Chemical Engineering Communications* **2017**, *204*, 689–697, doi:10.1080/00986445.2017.1306518.

15. Lütke, S.F.; Igansi, A. V; Pegoraro, L.; Dotto, G.L.; Pinto, L.A.A.; Cadaval, T.R.S. Preparation of activated carbon from black wattle bark waste and its application for phenol adsorption. *Journal of Environmental Chemical Engineering* **2019**, *7*, 103396, doi:10.1016/j.jece.2019.103396.

16. de Oliveira, G.F.; de Andrade, R.C.; Trindade, M.A.G.; Andrade, H.M.C.; Teodoro de Carvalho, C. Thermogravimetric and spectroscopic study (TG–DTA/FT–IR) of activated carbon from the renewable biomass source Babassu. *Química Nova* **2016**, doi:10.21577/0100-4042.20160191.

17. Uğurlu, M.; Gürses, A.; Açıkyıldız, M. Comparison of textile dyeing effluent adsorption on commercial activated carbon and activated carbon prepared from olive stone by ZnCl2 activation. *Microporous and Mesoporous Materials* **2008**, *111*, 228–235, doi:10.1016/j.micromeso.2007.07.034.

18. Ugurlu, M.; Yilmaz, S.I.; Vaizogullar, A. Removal of Color and COD from Olive Wastewater by Using Three-Phase Three-Dimensional (3D) Electrode Reactor. *Materials Today: Proceedings* **2019**, *18*, 1986–1995, doi:10.1016/j.matpr.2019.06.690.

19. Renault, F.; Morin-Crini, N.; Gimbert, F.; Badot, P.-M.; Crini, G. Cationized starch-based material as a new ion-exchanger adsorbent for the removal of C.I. Acid Blue 25 from aqueous solutions. *Bioresource Technology* **2008**, *99*, 7573–7586, doi:10.1016/j.biortech.2008.02.011.